SHAN: Object-Level Privacy Detection via Inference on Scene Heterogeneous Graph

Zhuohang Jiang[1*], Bingkui Tong[2*], Xia Du[3], Ahmed Alhammadi[4], and Jizhe Zhou[5]

[1] Sichuan University jzh@stu.scu.edu.cn
[2] Sichuan University tongbingkui@stu.scu.edu.cn
[3] Xiamen University of Technology duxia@xmut.edu.cn
[4] Mohamed Bin Zayed University for Humanities ahmad.khayyat@gmail.com
[5] Sichuan University jzzhou@scu.edu.cn

Abstract. With the rise of social platforms, protecting privacy has become an important issue. Privacy object detection aims to accurately locate private objects in images. It is the foundation of safeguarding individuals' privacy rights and ensuring responsible data handling practices in the digital age. Since privacy of object is not shift-invariant, the essence of the privacy object detection task is inferring object privacy based on scene information. However, privacy object detection has long been studied as a subproblem of common object detection tasks. Therefore, existing methods suffer from serious deficiencies in accuracy, generalization, and interpretability. Moreover, creating large-scale privacy datasets is difficult due to legal constraints and existing privacy datasets lack label granularity. The granularity of existing privacy detection methods remains limited to the image level. To address the above two issues, we introduce two benchmark datasets for object-level privacy detection and propose SHAN, Scene Heterogeneous graph Attention Network, a model constructs a scene heterogeneous graph from an image and utilizes self-attention mechanisms for scene inference to obtain object privacy. Through experiments, we demonstrated that SHAN performs excellently in privacy object detection tasks, with all metrics surpassing those of the baseline model.

Keywords: Object-Level Privacy Detection · Scene Inference · Scene Heterogeneous Graph

1 Introduction

The privacy object detection task aims to enable models to accurately localize privacy-sensitive objects in an image. Researching this problem is of significant importance for achieving personal privacy protection in network images and videos. With the advent of the digital media era, an increasing number of people are choosing to share photos and videos on social media platforms [15, 39]

* These authors contributed equally to this work.

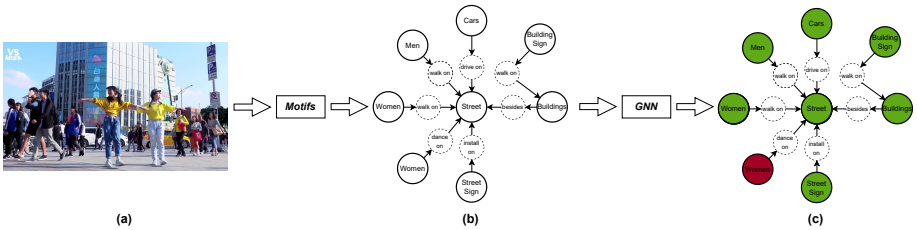

Fig. 1: (a) Example image (b) SHAN generates scene heterogeneous graph based on scene information, where solid nodes and dashed nodes correspond to object nodes and relation nodes respectively. (c) Inference results of SHAN, where red and green correspond to privacy nodes and non-privacy nodes respectively.

such as Instagram, Facebook, etc., making images and videos the primary form of information dissemination. As the form of information dissemination gradually shifts from text to images, images and videos on the internet are becoming increasingly abundant, leading to a proliferation of privacy infringements in online videos and images [38]. For example, in some street interview videos, there may be a large number of facial images of passersby, and the publication of such videos often inadvertently violates the privacy rights of those passersby. Therefore, the protection of user privacy has received a considerable amount of attention. The Privacy-Net [12] proposed by Bach Ngoc Kim et al. encodes images to obfuscate privacy information while retaining essential information for specific tasks. The DeepPrivacy model [9] proposed by Håkon Hukkelås et al. ensures complete anonymization of all faces in images by generating images based on privacy-sensitive information using generative adversarial networks [5].

The rise and dissemination of such multimedia content pose significant challenges to content regulation [19, 22], particularly in terms of privacy protection. Without proper control over the dissemination of private content, it not only compromises individual privacy and security but also brings certain risks and challenges to society. Therefore, strengthening privacy protection related to network images and videos has become an urgent task, and promoting the development of privacy object detection technology has become increasingly imperative.

Privacy object detection technology has received significant attention in recent years. Mohamed Moustafa utilized a convolutional neural network model [14] to construct a classifier for categorizing pornographic data, enabling the classification of pornographic images. Lam Tran et al. proposed the Privacy-CNH framework [26], which utilizes hierarchical features in deep learning models to detect photos with privacy risks. Ashwini Tonge et al. used a convolutional neural network to build an image privacy prediction model [25] that automatically analyzes the content and context information of images, thereby predicting the level of privacy in the images and assisting users in assessing privacy risks. Xin Jin et al. employed a convolutional neural network framework [11] to classify pornographic and normal images.

However, the aforementioned research [12, 26] focuses only on image-level assessment and cannot perform object-level privacy judgment. This limitation results in numerous meaningful images being unable to be shared online due to containing small portions of private content. Privacy object detection technology with object-level accuracy can identify the privacy-sensitive areas in images and apply pixelation, allowing for the free distribution of images while maintaining privacy. Therefore, extending privacy detection technology to the object level holds significant importance. However, research on object-level privacy detection is limited, with only Jun Yu et al. attempting to use deep convolutional neural networks and tree classifiers [34] to detect privacy-sensitive object classes. However, this method only considers visual features and ignores scene information, resulting in mediocre performance.

The privacy of objects does not possess shift invariance, meaning privacy varies with the position of objects within the image. Therefore, we propose a new perspective in this paper: privacy object detection is essentially a process of inferring object privacy based on scene information. For example, in Fig. 1.a, we can infer from the scene information that the dancing woman is the main focus and lacks privacy, while pedestrians, road signs, and other objects are considered privacy-sensitive objects.

The privacy object detection problem has long been regarded as a subset of object detection [9, 12, 14], leading to current methods primarily relying on traditional object detection methods. These methods depend on visual features for detection, lacking scene reasoning capabilities. Consequently, they struggle to address the challenge that privacy objects do not exhibit shift invariance. As a result, these methods often exhibit lower detection accuracy, poor generalization, and limited interpretability.

Furthermore, constrained by ethical and legal considerations, creating large-scale privacy datasets is exceptionally challenging. Existing small-scale privacy datasets often only provide labels at the image level. As a result, current methods can only perform privacy judgments at the image level and cannot achieve object-level privacy judgment.

To address the limitations of existing privacy object detection methods, we first manually annotated and generated two object-level benchmark privacy datasets. These datasets consist of approximately fifteen thousand images, filling the gap in the field's dataset availability. Moreover, we propose SHAN: Scene Heterogeneous graph Attention Network. It can obtain comprehensive scene information by constructing a scene heterogeneous graph and utilize self-attention mechanisms on this graph to infer the privacy of all object nodes within it.

Our main contributions can be summarized as follows:

- We elucidate that privacy object detection is essentially a process of inferring object privacy based on scene information.
- We propose the SHAN model, which elevates the granularity of privacy object detection to the object level and exhibits outstanding performance in terms of accuracy, generalization, and interpretability.
- We create two benchmark datasets for object-level privacy detection.

2 Related Work

2.1 Privacy Image Protection

With the rapid growth of image data and the persistent risk of personal privacy information leakage, safeguarding users' privacy image information has become an urgent challenge in the fields of computer science and information security [1, 2]. This challenge has attracted widespread attention and relentless efforts from numerous researchers. Privacy image protection utilizes techniques such as machine learning to automatically identify and process privacy regions in images to effectively protect user privacy. Protection methods typically involve blurring, mosaic, or masking sensitive areas to ensure that privacy regions are not directly exposed when sharing or publishing images. For example, the Privacy-CNH [26] model proposed by Lam Tran and colleagues employs deep learning models to detect photos with privacy risks, thereby safeguarding user privacy. However, most current models are limited to image-level privacy detection and pay less attention to object-level privacy detection models. Only Jun Yu [34] and others have attempted to detect privacy-sensitive object classes at the object level using deep convolutional neural networks and tree classifiers.

2.2 Scene Graph Generation

Scene graphs [33, 40] provide a structured representation of a scene, articulating the attributes of objects and relationships between them. Given an image, scene graph generation [31, 33] allow for the identification of object positions, categories, and inter-object relationships. Scene graph generation models typically consist of two main components: object detection modules and relationship prediction modules. The object detection module identifies objects within the image, while the relationship prediction module infers relationships between objects based on features detected by the object detection module. The output of scene graph generation models is generally represented as a triple $< subject, predicate, object >$. For instance, Kaihua Tang et al. proposed a dynamic visual context tree model, VCTree [24], which effectively captures parallel and hierarchical relationships between objects. Furthermore, it adapts its structure and generates scene graphs adaptively based on different images and tasks.

2.3 Graph Neural Networks

Graph Neural Networks (GNNs) [37] are a class of machine learning and deep learning methods designed for graph-structured data. With the widespread application of graph data in various fields, GNNs have gradually become a research hotspot, attracting significant attention and research efforts from both academia and industry. GNNs effectively capture the topological structure and node features of graph data, enabling tasks such as node and edge classification, prediction, and clustering. Early GNN models focused on learning low-dimensional representations of nodes, with representative models including DeepWalk [16]

and node2vec [6]. These models utilize methods based on random walks and node neighborhood sampling to represent the connections between nodes. Currently, prominent GNN models include GCN [13], GAT [27], GraphSAGE [7], and GIN [32], which utilize information propagation to convey relational information between nodes and accomplish inference tasks. Due to the prevalence of discrete information in real-world scenarios, and GNNs' capability to handle such data, they have wide-ranging applications in social networks, recommendation systems, bioinformatics, chemistry, transportation, and other fields.

2.4 Heterogeneous Graphs

Heterogeneous graphs [28] consist of nodes and edges of different types. In reality, there are many graph networks composed of nodes of different types, such as social networks and scene graphs, which can be effectively represented using heterogeneous graphs. Common heterogeneous graph models include HetGNN [36] (Heterogeneous Graph Neural Network), HAN [29] (Heterogeneous Graph Attention Network), Heterogeneous graph propagation network [10] and Heterogeneous graph transformer [8]. These models have achieved good performance on various heterogeneous graph datasets and are widely applied in social network analysis [3], recommendation systems [21], knowledge graphs [30], and other domains.

3 Method

In Sec 1, it is noted that the privacy object detection problem has long been regarded as a subset of object detection, resulting in poor performance of current privacy object detection methods [9,34]. However, privacy object detection is essentially a process of inferring the privacy of objects based on scene information. In this chapter, we introduce our method: SHAN, which is a universal privacy object detection model combining scene heterogeneous graphs [40] and graph neural networks [32]. The structure of the SHAN model, which can be divided into two parts: the scene heterogeneous graph generation module and the scene heterogeneous graph-based inference module (Fig. 2). The scene heterogeneous graph generation module extracts objects and their relationships in the image, generating a heterogeneous graph containing two different types of nodes: object nodes and relationship nodes. The inference module uses a heterogeneous graph attention network to infer the heterogeneous graph containing scene information, ultimately determining the privacy of each object node. With SHAN, we can obtain scene information from images and infer the privacy of objects in the scene, thereby completing the task of privacy object detection.

3.1 Scene Graph Generation

To obtain scene information, we adopted the pre-trained Casual-MOTIFS [23] model, a novel architecture designed to capture higher-order patterns in scene

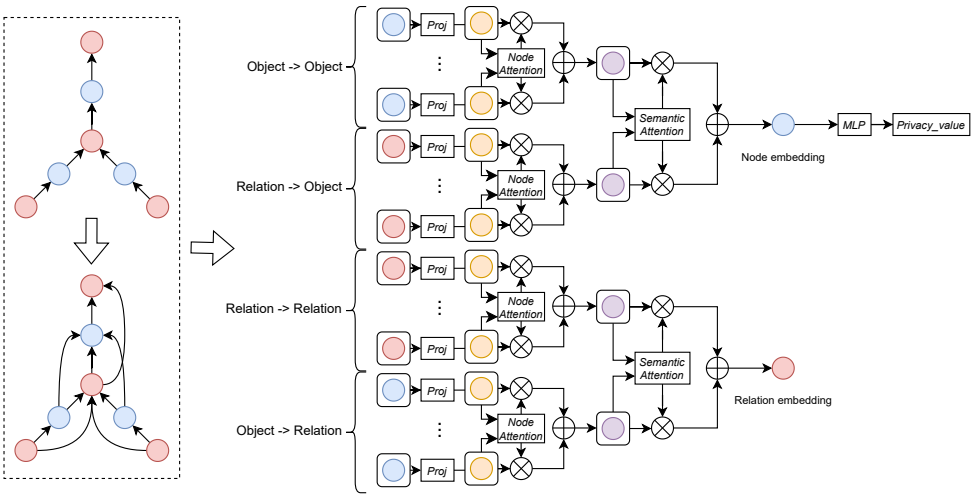

Fig. 2: Overview diagram of the second part of SHAN: the heterogeneous graph attention neural network model, which is responsible for transmitting information between nodes, conducting inference, and ultimately determining whether it is a private node.

graphs. The scene graph generated by the Casual-MOTIFS model [35] contains two types of information: node features o and relationships r between nodes. Traditional homogeneous graph networks cannot simultaneously represent node and relationship information, whereas heterogeneous graphs can contain nodes of various types. Therefore, we consider the relationships in the generated scene graph as a new type of node, thus forming a heterogeneous graph composed of (o, r) pairs, where o represents Object Node and r represents Relation Node.

3.2 Heterogeneous Graph Attention Network

After constructing the heterogeneous graph based on scene information, we utilize a heterogeneous graph attention neural network to generate privacy vectors for each node, followed by generating corresponding privacy values through an MLP.

The heterogeneous graph attention neural network [29] consists of three steps:

1. Pruning the constructed heterogeneous graph and adding relevant edges accordingly.
2. Applying node-level attention to identical node-paths.
3. Applying semantic-level attention to different node-paths to generate privacy feature vectors for each node, which are then used to generate privacy values through an MLP.

Pruning and Adding Relevant Edges Through the scene graph generation model, we obtain the set of object nodes $O = \{o_1, o_2, ..., o_i\}$, the set of relationship nodes $R = \{r_1, r_2, ..., r_j\}$, as well as the connection information between

object nodes and relationship nodes $L = \{(o_i, r_j), (o_k, r_l), ...\}$ and the confidence scores for connections $T = \{t_1, t_2, ...\}$. During this process, nodes with connection confidence scores t_i lower than 0.5 are removed to reduce redundancy in the scene information.

Additionally, when connections like $o_i \to r \to o_j$ exist, we add a connection $o_i \to o_j$; when connections like $r_i \to o \to r_j$ exist, we add a connection $r_i \to r_j$. This operation extends the information flow paths between nodes and relationships, enhancing the channels for information propagation and thus improving the efficiency of node information retrieval. Consequently, the connection structure of nodes expands from the original two types to four types.

$$(o \to r, r \to o) \Rightarrow (o \to r, r \to o, r \to r, o \to o) \tag{1}$$

Node-Level Attention In the generated heterogeneous graph, we consider four types of node-paths: $(o \to r, r \to o, r \to r, o \to o)$. For each node-path, we conduct attention convolution operations on graph nodes to generate feature vectors for different node-paths.

Node Feature Transformation: Initially, for object nodes o and r, we conduct feature transformations separately using feature matrices W_1 and W_2.

$$\begin{cases} \hat{o_i} = W_1 \cdot o_i \\ \hat{r_i} = W_2 \cdot r_i \end{cases} \tag{2}$$

Attention Weight Calculation: Next, for nodes along the same path, we conduct attention operations. For object nodes, we need to compute attention information $e_{o_i}^{o_j}$ for node pairs $o_j \to o_i$ along the path $o \to o$, and simultaneously, for node pairs $r_j \to o_i$ along the path $r \to o$, we compute attention information $e_{o_i}^{r_j}$.

$$\begin{cases} e_{o_i}^{o_j} = att_{node}\left(\hat{o_i}, \hat{o_j}, o \to o\right) \\ e_{o_i}^{r_j} = att_{node}\left(\hat{o_i}, \hat{r_j}, r \to o\right) \end{cases} \tag{3}$$

Following that, we apply a softmax operation to the attention information $e_{o_i}^{o_j}$ and $e_{o_i}^{r_j}$ to obtain the attention weight $\alpha_{o_i}^{o_j}$ and $\alpha_{o_i}^{r_j}$.

$$\begin{cases} \alpha_{o_i}^{o_j} = softmax\left(e_{o_i}^{o_j}\right) = \frac{\exp(\sigma(a_{o\to o} \cdot (\hat{o_i} \otimes \hat{o_j})))}{\sum_{m \in P_{o_i}^{o}} \exp(\sigma(a_{o\to o} \cdot (\hat{o_i} \otimes \hat{o_m})))} \\ \alpha_{o_i}^{r_j} = softmax\left(e_{o_i}^{r_j}\right) = \frac{\exp(\sigma(a_{r\to o} \cdot (\hat{o_i} \otimes \hat{r_j})))}{\sum_{m \in P_{o_i}^{r}} \exp(\sigma(a_{r\to o} \cdot (\hat{o_i} \otimes \hat{r_m})))} \end{cases} \tag{4}$$

Furthermore, for relation nodes, we also need to compute attention information $e_{r_i}^{r_j}$ for node pairs $r_j \to r_i$ along the path $r \to r$, and simultaneously, for node pairs $o_j \to r_i$ along the path $o \to r$, we compute attention information $e_{r_i}^{o_j}$.

$$\begin{cases} e_{r_i}^{r_j} = att_{node}\left(\hat{r_i}, \hat{r_j}, r \to r\right) \\ e_{r_i}^{o_j} = att_{node}\left(\hat{r_i}, \hat{o_j}, o \to r\right) \end{cases} \tag{5}$$

Following that, we apply a softmax operation to the attention information $e_{r_i}^{o_j}$ and $e_{r_i}^{r_j}$ to obtain the attention weight $\alpha_{r_i}^{o_j}$ and $\alpha_{r_i}^{r_j}$.

$$\begin{cases} \alpha_{r_i}^{r_j} = softmax\left(e_{r_i}^{r_j}\right) = \frac{\exp(\sigma(a_{r\to r}\cdot(\hat{r_i}\otimes\hat{r_j})))}{\sum_{m\in P_{r_i}^r}\exp(\sigma(a_{r\to r}\cdot(\hat{r_i}\otimes\hat{r_m})))} \\ \alpha_{r_i}^{o_j} = softmax\left(e_{r_i}^{o_j}\right) = \frac{\exp(\sigma(a_{o\to r}\cdot(\hat{r_i}\otimes\hat{o_j})))}{\sum_{m\in P_{r_i}^o}\exp(\sigma(a_{o\to r}\cdot(\hat{r_i}\otimes\hat{o_m})))} \end{cases} \tag{6}$$

Compute Node-Level Attention Values: Finally, within the same pathway, we multiply each connected feature vector M_m by the corresponding attention weight and sum them to generate a feature vector. For each object node o_i, we obtain a set of feature vectors $\left\{z_{o_i}^o, z_{o_i}^r\right\}$, and for each relation node r_i, we obtain a set of feature vectors $\left\{z_{r_i}^o, z_{r_i}^r\right\}$. Here, $z_{M_i}^N$ represents the node feature after attention weight summation, and $\alpha_{M_m}^{N_i}$ represents the attention weight for each connected feature, where M_m denotes the connected feature vector.

$$\begin{cases} z_{o_i}^o = \sigma\left(\sum_{m\in P_{o_i}^o}\alpha_{o_i}^{o_m}\cdot\hat{o_m}\right) \\ z_{o_i}^r = \sigma\left(\sum_{m\in P_{o_i}^r}\alpha_{o_i}^{r_m}\cdot\hat{r_m}\right) \\ z_{r_i}^r = \sigma\left(\sum_{m\in P_{r_i}^r}\alpha_{r_i}^{r_m}\cdot\hat{r_m}\right) \\ z_{r_i}^o = \sigma\left(\sum_{m\in P_{r_i}^o}\alpha_{r_i}^{o_m}\cdot\hat{o_m}\right) \end{cases} \tag{7}$$

Semantic-Level Attention We use attention networks to synthesize semantic information for paths with the same node categories but different node-paths, allocating different parameters to different node-paths. The purpose is to allow object nodes to gather features of adjacent relationships while also obtaining features of adjacent object nodes. In this way, we can infer the environmental information of each node through adjacent features and relationship nodes, ultimately generating an embedding vector for each node.

Node-Path Feature Transformation: Firstly, for different path features $z_{o_i}^o$, $z_{o_i}^r$, $z_{r_i}^o$, $z_{o_i}^r$, we perform feature transformation separately using feature matrices W_3, W_4, W_5, and W_6.

$$\begin{cases} z_{o_i}^{\hat{o}} = W_3\cdot z_{o_i}^o \\ z_{o_i}^{\hat{r}} = W_4\cdot z_{o_i}^r \\ z_{r_i}^{\hat{o}} = W_5\cdot z_{r_i}^o \\ z_{r_i}^{\hat{r}} = W_6\cdot z_{r_i}^r \end{cases} \tag{8}$$

Attention Weight Calculation: Then, we compute the attention weight information w_{κ_i} between different paths, then normalize these weights to calculate the attention weights $\beta_{\kappa i}$. For object nodes o, we need to integrate and compute the attention information w_o^o and w_o^r for both paths $o\to o$ and $r\to o$.

$$\begin{cases} w_o^o = \frac{1}{|\mathcal{V}|}\sum_{j\in\mathcal{V}} q^T\cdot\tanh\left(W\cdot z_{o_j}^{\hat{o}} + b\right) \\ w_o^r = \frac{1}{|\mathcal{V}|}\sum_{j\in\mathcal{V}} q^T\cdot\tanh\left(W\cdot z_{o_j}^{\hat{r}} + b\right) \end{cases} \tag{9}$$

Then, we normalize the attention information w_o^o and w_o^r to obtain the attention weights β_o^o and β_o^r corresponding to the paths $o \to o$ and $r \to o$, respectively.

$$\begin{cases} \beta_o^o = \frac{\exp(w_o^o)}{\exp(w_o^o)+\exp(w_o^r)} \\ \beta_o^r = \frac{\exp(w_o^r)}{\exp(w_o^o)+\exp(w_o^r)} \end{cases} \tag{10}$$

For relation nodes r, we need to integrate and compute the attention information w_r^o and w_r^r for both paths $o \to r$ and $r \to r$.

$$\begin{cases} w_r^o = \frac{1}{|\mathcal{V}|} \sum_{j \in \mathcal{V}} q^T \cdot \tanh\left(W \cdot z_{r_j}^{\hat{o}} + b\right) \\ w_r^r = \frac{1}{|\mathcal{V}|} \sum_{j \in \mathcal{V}} q^T \cdot \tanh\left(W \cdot z_{r_j}^{\hat{r}} + b\right) \end{cases} \tag{11}$$

Then, we normalize the attention information w_r^o and w_r^r to obtain the attention weights β_r^o and β_r^r corresponding to the paths $o \to r$ and $r \to r$, respectively.

$$\begin{cases} \beta_r^o = \frac{\exp(w_r^o)}{\exp(w_r^o)+\exp(w_r^r)} \\ \beta_r^r = \frac{\exp(w_r^r)}{\exp(w_r^o)+\exp(w_r^r)} \end{cases} \tag{12}$$

In this process, W represents the weight matrix, $z_{\kappa_i}^{N_j}$ represents the feature information obtained in the previous stage, b is the bias, and V represents the number of nodes.

Compute Semantic-Level Attention Values: Next, for the feature vectors obtained in the previous step, we apply the attention weight β_{κ_i} operation on different paths to generate the feature information Z_{o_i} for each node and the feature information Z_{r_i} for each path.

$$\begin{cases} Z_{o_i} = \sigma\left(\beta_o^o \cdot z_{o_i}^{\hat{o}} + \beta_o^r \cdot z_{o_i}^{\hat{r}}\right) \\ Z_{r_i} = \sigma\left(\beta_r^o \cdot z_{r_i}^{\hat{o}} + \beta_r^r \cdot z_{r_i}^{\hat{r}}\right) \end{cases} \tag{13}$$

We repeat the above steps using multiple heterogeneous graph attention neural networks [29] for information propagation to collect information from more distant nodes and relationships.

Compute the Privacy Value for Each Node: Finally, we apply a multilayer perceptron (MLP) to each embedding vector, and finally use the output privacy confidence to determine whether a node is a privacy node. Here, $is\_privacy_{o_i}$ represents the privacy level of node o_i.

$$is\_privacy_{o_i} = sigmod(W \cdot Z_{o_i} + b) \tag{14}$$

4 Experiments

4.1 Dataset Introduction

In this subsection, we will introduce the creation of two datasets.

The **MOSAIC** dataset contains 13,384 images re-generated by AIGC [20], which contain images of different categories of private objects such as people's

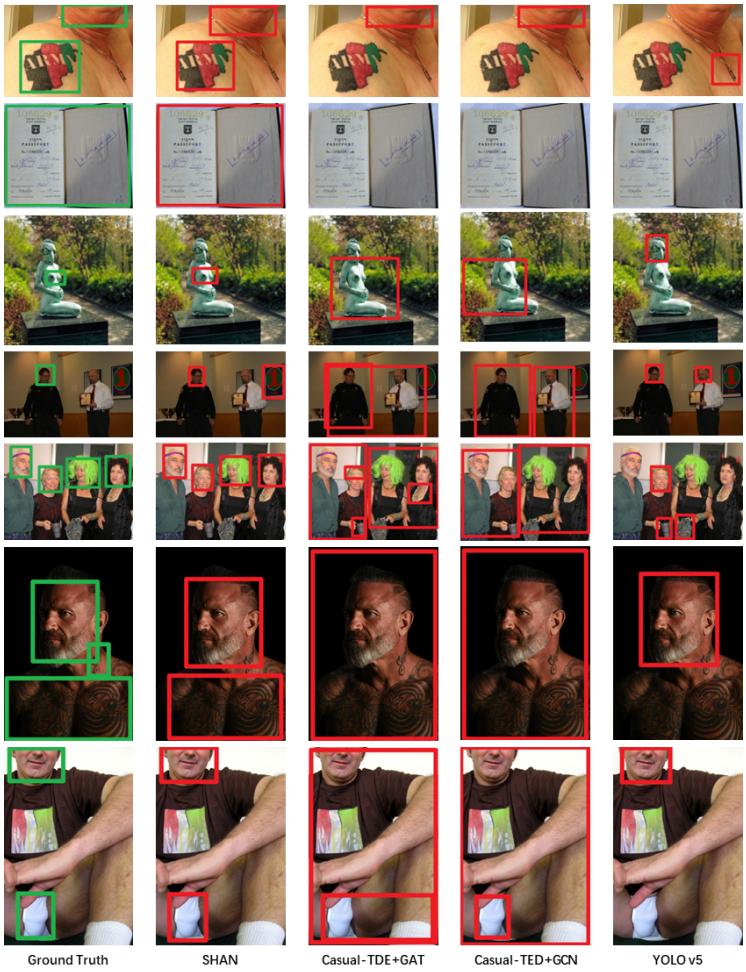

Fig. 3: The image illustrates partial results of SHAN, SGAT, SGCN, and YOLO v5 models evaluated on the PRIVACY1000, juxtaposed with Ground Truth for comparison.

faces, body parts, bloody violence, transcripts, license plate slogans. Compared to other datasets, our dataset achieves node-level accuracy while removing real privacy information.

The **PRIVACY1000** dataset contains 1000 manually labeled real-world images of private body parts, human faces, fancy clothes, bloody photos, political slogans, license plate messages. Compared to the MOSAIC dataset, it has more categories of private content, while not having been generated by AIGC, and has relatively good authenticity.

4.2 Dataset Collection

Because of the current restrictions on privacy data collection by laws and regulations around the world, a node-level privacy object detection dataset does not currently exist. Therefore, we circumvent the restriction of privacy data collection by the following methods to produce two datasets, MOSAIC and PRIVACY1000. The production of MOSAIC follows the following steps:

Fig. 4: The figure shows photos in our two datasets. **First Row**: PRIVACY1000. **Second Row**: MOSAIC.

1. **Collect Private Images**: We generally believe that images with mosaics are often images with private objects, and the location of the mosaics is the location of the private objects. Therefore, we downloaded dozens of hours of videos(*Guardians of Liberation West*) with mosaic content and sliced them frame by frame to save images with mosaic content.
2. **Identify and Locate the Position of Mosaics**: A target detection algorithm is used to identify the number and location of mosaics in the image, deduct the mosaic part of the image, and save the number and location of the mosaics at the same time.
3. **Recover the Deducted Part by AIGC**: Since directly collecting private pictures may violate some laws and regulations, we can collect private pictures without collecting real private data by deducting the mosaic part and then completing it by AIGC [20].

Through this process, we created a object-level privacy dataset containing over 13,000 images without privacy infringement. This approach may have some errors, as in some cases, the mosaic may include objects such as blood, pornography, rather than privacy-related objects. Therefore, to test the model more accurately, we collected images containing privacy objects from *Flicker* and manually labeled the privacy objects in them, creating the PRIVACY1000 dataset containing 1000 images. To protect privacy, we will not open-source the PRIVACY1000 dataset.

4.3 Experimental Setup

In our experimental setup, we utilized the PRIVACY1000 dataset for model training and the MOSAIC dataset to test the model's generalization capabilities. We randomly partitioned 80% of the PRIVACY1000 dataset as the training set and 20% as the validation set. And we selected YOLOv5 [17] and Faster RCNN [18], which have demonstrated excellent performance in the traditional object detection domain, as the baseline models for our experiment.

4.4 Ablation Experiments

In order to deeply understand the contributions of different modules to the performance of the SHAN model, we made a series of modifications. To explore the impact of the heterogeneous graph structure, we replaced the HAN [29] module (heterogeneous graph attention network) in SHAN with GAT [27] (homogeneous graph attention network), which prevents the model from capturing the relationship information among objects in the scene. Based on this, we further replaced the GAT [27] module with GCN [13] (homogeneous graph convolution network) to study the impact of the attention mechanism. To assess the influence of the quality of scene graphs on the model performance, we replaced the scene graph generation module in SHAN from Casual-MOTIFS [23] to the slightly less performant RelTR [4].

We randomly split the Privacy1000 dataset, with 80% used for training and 20% for testing. We measured the Precision, Recall, and F1 score of the SHAN model with different module modifications, to evaluate the impact of each modification on the model performance.

4.5 Robustness Experiments

To further test the robustness of SHAN, we performed each one of the following three processing methods on each image in the test set of the PRIVACY1000 dataset, and tested it on the trained SHAN model:

- **Rotation**: We applied random rotation to the input image, with the rotation angle adjusted between -30 degrees and 30 degrees.
- **Masking**: We randomly selected two to three points on the input image, and then masked the area with these selected points as the center and a side length of 20 pixels.
- **Scaling**: We applied random scaling to the selected image, with the scaling ratio varying between 0.8 and 1.2.

This processing method aims to simulate various image changes that may be encountered in the real world, thereby more comprehensively evaluating the robustness and adaptability of the model

Table 1: The table below shows experiment results for the two privacy datasets of different algorithms.

	PRIVACY1000			MOSAIC		
Methods	Precision	Recall	F1 Score	Precision	Recall	F1 Score
Faster-RCNN [18]	0.7192	0.4981	0.5886	0.2917	0.2662	0.2784
YoloV5x [17]	0.8667	0.6634	0.7515	0.4323	0.3543	0.3894
SHAN	**0.9723**	**0.9165**	**0.9436**	**0.9349**	**0.9546**	**0.9447**

Table 2: The table below shows experiment results for ablation experiments.

Methods	Precision	Recall	F1 score
RelTR [4]+GCN [13]	0.8634	0.8723	0.8678
RelTR [4]+GAT [27]	0.8692	0.8654	0.8673
RelTR [4]+HAN [29]	0.8975	0.8798	0.8886
Casual-MOTIFS [23]+GCN [13]	0.9011	0.8786	0.8902
Casual-MOTIFS [23]+GAT [27]	0.9552	0.8697	0.9104
SHAN	**0.9723**	**0.9165**	**0.9436**

Table 3: The table below shows experiment results for robust experiments.

Augmentation Methods	Precision	Recall	F1 score
Rotation	0.8939	0.9351	0.9141
Zoom	0.8911	0.9355	0.9128
Masking	0.8629	0.9400	0.8998
Origin	**0.9723**	**0.9165**	**0.9436**

4.6 Result and Discussion

Tab. 1 displays the performance of SHAN and baseline models on the PRIVACY1000 dataset, as well as their generalization performance on the MOSAIC dataset. Both baseline models, YOLOV5 [17] and Faster-RCNN [18], are traditional object detection methods relying on visual features. They lack the ability to infer based on scene information, and therefore perform poorly in terms of accuracy and generalization. SHAN builds scene heterogeneous graphs based on scene information and infers based on these graphs, outperforming the baseline models on all metrics.

Tab. 2 shows the results of the ablation experiments. The underperformance of Casual-MOTIFS [23]+GCN [13] can be attributed to its use of a homogeneous graph that fails to capture the relationships between objects in the scene. Moreover, its inference process relies on convolution rather than the attention mechanism, limiting the model's receptive field and making it difficult to capture long-distance dependencies. Although Casual-MOTIFS [23]+GAT [27] introduces the attention mechanism, its performance is still limited because it also infers pri-

vacy based on a homogeneous graph. By contrast, the SHAN model builds a scene heterogeneous graph to comprehensively capture scene information and uses a self-attention mechanism for inference based on this, outperforming all other methods. Notably, even though it is Casual-MOTIFS [23]+GCN [13], its performance still exceeds that of the baseline models, which primarily detect based on visual features. This further confirms the point we propose in this paper, namely, that the essence of privacy object detection is to infer the privacy of objects based on scene information.

Furthermore, we can draw the following conclusion from Tab. 2: The effectiveness of methods that infer based on scene heterogeneous graphs largely depends on the completeness of scene information. When we replace Casual-MOTIFS [23] with RelTR [4] in the scene graph generation module, the quality of the generated scene graph declines, leading to incomplete scene information. This incomplete scene information further affect the results of inference based on it.

Tab. 3 further corroborates this conclusion. When SHAN faces modifications like rotation and scaling that have less impact on scene information, its performance is not greatly affected. However, when SHAN encounters changes like masking that could have a significant impact on scene information (for example, masking some key objects, leading to a loss of scene information), its overall performance drops dramatically.

5 Conclusion

Given that the privacy of objects do not possess shift invariance, we cannot simply regard the privacy object detection task as a traditional object recognition task. The privacy of objects needs to be inferred based on contextual information. Therefore, we propose a novel method to solve the privacy object detection task. This method transforms images into scene graphs containing scene objects and their relationships through a scene graph generation model, and then infers the privacy of object nodes in the scene graph through a graph network. Compared with existing methods, this method has better interpretability and can achieve object-level privacy judgments. Based on this, we propose the SHAN model. To further support research in this field, we created two object-level benchmark privacy datasets: PRIVACY1000 and MOSAIC, through manual annotation and image generation respectively, to fill the gap in datasets in this field. SHAN performs excellently on these two datasets, with an precision of 97% on PRIVACY1000, and outperforms the benchmark models on all evaluation metrics. In addition, this model can not only be used to solve the privacy object detection task, but also to solve other problems based on scene inference, such as violence and softcore pornography content detection. It has broad application prospects and will be the direction of our future research.

References

1. Adams, A., Angela Sasse, M.: Privacy in multimedia communications: Protecting users, not just data. In: People and computers XV—interaction without frontiers: Joint Proceedings of HCI 2001 and IHM 2001. pp. 49–64. Springer (2001)
2. Bellotti, V.: Design for privacy in multimedia computing and communications environments. Technology and privacy: The new landscape pp. 63–98 (1998)
3. Cai, D., Shao, Z., He, X., Yan, X., Han, J.: Mining hidden community in heterogeneous social networks. In: Proceedings of the 3rd international workshop on Link discovery. pp. 58–65 (2005)
4. Cong, Y., Yang, M.Y., Rosenhahn, B.: Reltr: Relation transformer for scene graph generation. IEEE Transactions on Pattern Analysis and Machine Intelligence (2023)
5. Creswell, A., White, T., Dumoulin, V., Arulkumaran, K., Sengupta, B., Bharath, A.A.: Generative adversarial networks: An overview. IEEE signal processing magazine **35**(1), 53–65 (2018)
6. Grover, A., Leskovec, J.: node2vec: Scalable feature learning for networks. In: Proceedings of the 22nd ACM SIGKDD international conference on Knowledge discovery and data mining. pp. 855–864 (2016)
7. Hamilton, W., Ying, Z., Leskovec, J.: Inductive representation learning on large graphs. Advances in neural information processing systems **30** (2017)
8. Hu, Z., Dong, Y., Wang, K., Sun, Y.: Heterogeneous graph transformer. In: Proceedings of the web conference 2020. pp. 2704–2710 (2020)
9. Hukkelås, H., Mester, R., Lindseth, F.: Deepprivacy: A generative adversarial network for face anonymization (2019)
10. Ji, H., Wang, X., Shi, C., Wang, B., Philip, S.Y.: Heterogeneous graph propagation network. IEEE Transactions on Knowledge and Data Engineering **35**(1), 521–532 (2021)
11. Jin, X., Wang, Y., Tan, X.: Pornographic image recognition via weighted multiple instance learning. IEEE Transactions on Cybernetics **49**(12), 4412–4420 (2019). https://doi.org/10.1109/TCYB.2018.2864870
12. Kim, B.N., Dolz, J., Jodoin, P.M., Desrosiers, C.: Privacy-net: An adversarial approach for identity-obfuscated segmentation of medical images (2020)
13. Kipf, T.N., Welling, M.: Semi-supervised classification with graph convolutional networks. arXiv preprint arXiv:1609.02907 (2016)
14. Moustafa, M.: Applying deep learning to classify pornographic images and videos (2015)
15. Nov, O., Naaman, M., Ye, C.: Motivational, structural and tenure factors that impact online community photo sharing. In: Proceedings of the International AAAI Conference on Web and Social Media. vol. 3, pp. 138–145 (2009)
16. Perozzi, B., Al-Rfou, R., Skiena, S.: Deepwalk: Online learning of social representations. In: Proceedings of the 20th ACM SIGKDD international conference on Knowledge discovery and data mining. pp. 701–710 (2014)
17. Redmon, J., Divvala, S., Girshick, R., Farhadi, A.: You only look once: Unified, real-time object detection. In: Proceedings of the IEEE conference on computer vision and pattern recognition. pp. 779–788 (2016)
18. Ren, S., He, K., Girshick, R., Sun, J.: Faster r-cnn: Towards real-time object detection with region proposal networks. Advances in neural information processing systems **28** (2015)

19. Ribaric, S., Ariyaeeinia, A., Pavesic, N.: De-identification for privacy protection in multimedia content: A survey. Signal Processing: Image Communication **47**, 131–151 (2016)
20. Rombach, R., Blattmann, A., Lorenz, D., Esser, P., Ommer, B.: High-resolution image synthesis with latent diffusion models. In: Proceedings of the IEEE/CVF conference on computer vision and pattern recognition. pp. 10684–10695 (2022)
21. Shi, C., Hu, B., Zhao, W.X., Philip, S.Y.: Heterogeneous information network embedding for recommendation. IEEE Transactions on Knowledge and Data Engineering **31**(2), 357–370 (2018)
22. Shu, X., Yao, D., Bertino, E.: Privacy-preserving detection of sensitive data exposure. IEEE transactions on information forensics and security **10**(5), 1092–1103 (2015)
23. Tang, K., Niu, Y., Huang, J., Shi, J., Zhang, H.: Unbiased scene graph generation from biased training. In: Proceedings of the IEEE/CVF conference on computer vision and pattern recognition. pp. 3716–3725 (2020)
24. Tang, K., Zhang, H., Wu, B., Luo, W., Liu, W.: Learning to compose dynamic tree structures for visual contexts. In: Proceedings of the IEEE/CVF conference on computer vision and pattern recognition. pp. 6619–6628 (2019)
25. Tonge, A., Caragea, C.: Image privacy prediction using deep neural networks (2019)
26. Tran, L., Kong, D., Jin, H., Liu, J.: Privacy-cnh: A framework to detect photo privacy with convolutional neural network using hierarchical features. In: Proceedings of the AAAI conference on artificial intelligence. vol. 30 (2016)
27. Velickovic, P., Cucurull, G., Casanova, A., Romero, A., Lio, P., Bengio, Y., et al.: Graph attention networks. stat **1050**(20), 10–48550 (2017)
28. Wang, X., Bo, D., Shi, C., Fan, S., Ye, Y., Philip, S.Y.: A survey on heterogeneous graph embedding: methods, techniques, applications and sources. IEEE Transactions on Big Data **9**(2), 415–436 (2022)
29. Wang, X., Ji, H., Shi, C., Wang, B., Ye, Y., Cui, P., Yu, P.S.: Heterogeneous graph attention network. In: The world wide web conference. pp. 2022–2032 (2019)
30. Wu, Y., Liu, X., Feng, Y., Wang, Z., Yan, R., Zhao, D.: Relation-aware entity alignment for heterogeneous knowledge graphs. arXiv preprint arXiv:1908.08210 (2019)
31. Xu, D., Zhu, Y., Choy, C.B., Fei-Fei, L.: Scene graph generation by iterative message passing. In: Proceedings of the IEEE conference on computer vision and pattern recognition. pp. 5410–5419 (2017)
32. Xu, K., Hu, W., Leskovec, J., Jegelka, S.: How powerful are graph neural networks? arXiv preprint arXiv:1810.00826 (2018)
33. Yang, J., Lu, J., Lee, S., Batra, D., Parikh, D.: Graph r-cnn for scene graph generation. In: Proceedings of the European conference on computer vision (ECCV). pp. 670–685 (2018)
34. Yu, J., Zhang, B., Kuang, Z., Lin, D., Fan, J.: iprivacy: image privacy protection by identifying sensitive objects via deep multi-task learning. IEEE Transactions on Information Forensics and Security **12**(5), 1005–1016 (2016)
35. Zellers, R., Yatskar, M., Thomson, S., Choi, Y.: Neural motifs: Scene graph parsing with global context. In: Proceedings of the IEEE conference on computer vision and pattern recognition. pp. 5831–5840 (2018)
36. Zhang, C., Song, D., Huang, C., Swami, A., Chawla, N.V.: Heterogeneous graph neural network. In: Proceedings of the 25th ACM SIGKDD international conference on knowledge discovery & data mining. pp. 793–803 (2019)
37. Zhang, Z., Cui, P., Zhu, W.: Deep learning on graphs: A survey. IEEE Transactions on Knowledge and Data Engineering **34**(1), 249–270 (2020)

38. Zhou, J., Pun, C.M.: Personal privacy protection via irrelevant faces tracking and pixelation in video live streaming. IEEE Transactions on Information Forensics and Security **16**, 1088–1103 (2020)
39. Zhou, J., Pun, C.M., Tong, Y.: Privacy-sensitive objects pixelation for live video streaming. In: Proceedings of the 28th ACM International Conference on Multimedia. pp. 3025–3033 (2020)
40. Zhu, G., Zhang, L., Jiang, Y., Dang, Y., Hou, H., Shen, P., Feng, M., Zhao, X., Miao, Q., Shah, S.A.A., et al.: Scene graph generation: A comprehensive survey. arXiv preprint arXiv:2201.00443 (2022)

Supplementary Materials: SHAN: Object-Level Privacy Detection via Inference on Scene Heterogeneous Graph

Zhuohang Jiang[1*], Bingkui Tong[2*], Xia Du[3], Ahmed Alhammadi[4], and Jizhe Zhou[5]

[1] Sichuan University jzh@stu.scu.edu.cn
[2] Sichuan University tongbingkui@stu.scu.edu.cn
[3] Xiamen University of Technology duxia@xmut.edu.cn
[4] Mohamed Bin Zayed University for Humanities ahmad.khayyat@gmail.com
[5] Sichuan University jzzhou@scu.edu.cn

In this supplementary material, we describe the methodology behind the creation of our MOSAIC dataset, as detailed in Section Sec. 1, and provide an overview of the PRIVACY1000 dataset in Section Sec. 2. We also explore the specifics of our implementation details and training procedures in Sections Sec. 3 and Sec. 4. We discuss the limitations of our study and the future research directions in Section Sec. 5.

1 MOSAIC Dataset Generation

Fig. 1: Some objects in MOSAIC.

* These authors contributed equally to this work.

The creation process of our MOSAIC dataset is divided into three stages:

1. In the first stage, we slice videos containing mosaics and save images with mosaics. During this stage, we chose "Guardians of the West" as the video source. "Guardians of the West" is a reality show of police documentary observation. Because it widely records the process of police handling illegal crimes, there are numerous mosaic areas covering different types of objects in the video, making it very suitable as a dataset for privacy object detection.
2. In the second stage, we use the YOLO model to train and recognize images with mosaic areas, then remove these areas in preparation for the regeneration of mosaic areas in the third step.
3. In the third stage, we use stable diffusion to regenerate the parts removed from the images, ultimately forming a complete privacy image that does not contain real privacy information. At the same time, through the position of the mosaic, we can accurately locate the privacy position in the image, thereby automatically completing the privacy object annotation task.

Through these three steps, we not only avoid the issue of being unable to publicly release the privacy image dataset due to the existence of real privacy and legal restrictions, but also solve the problem of lack of object-level datasets for privacy detection tasks, as we automatically annotate the privacy positions through the mosaic positions.

The MOSAIC dataset contains 13,384 images, covering 143 different object categories, including vehicles, noses, rooms, hats, trees, buildings, children, boxes, jeans, doors, signs, etc. These privacy nodes can be further divided into different categories, including human faces, body parts, bloody

2 PRIVACY1000 Dataset Generation

The PRIVACY1000 dataset is derived through manual screening and annotation of images from the Flickr image sharing platform. This dataset comprises 1000 images, each containing multiple manually annotated privacy objects. The dataset encompasses 144 different object categories, including arms, bags, books, boxes, heads, women, noses, etc. Compared to traditional privacy datasets, PRIVACY1000 enhances annotation granularity to the object level. Compared to the MOSAIC dataset, the content of the PRIVACY1000 dataset is more precise.

3 Implementation Details

3.1 Scene Heterogeneous Graph Generation

The scene graphs generated by our scene graph generation model contain the coordinates of numerous objects. To identify privacy objects, we compute the CIOU [1] (Complete Intersection over Union) between the coordinates of the annotated privacy objects and the generated objects in the scene graph. In this way, the objects with the highest CIOU [1] value are considered as the privacy

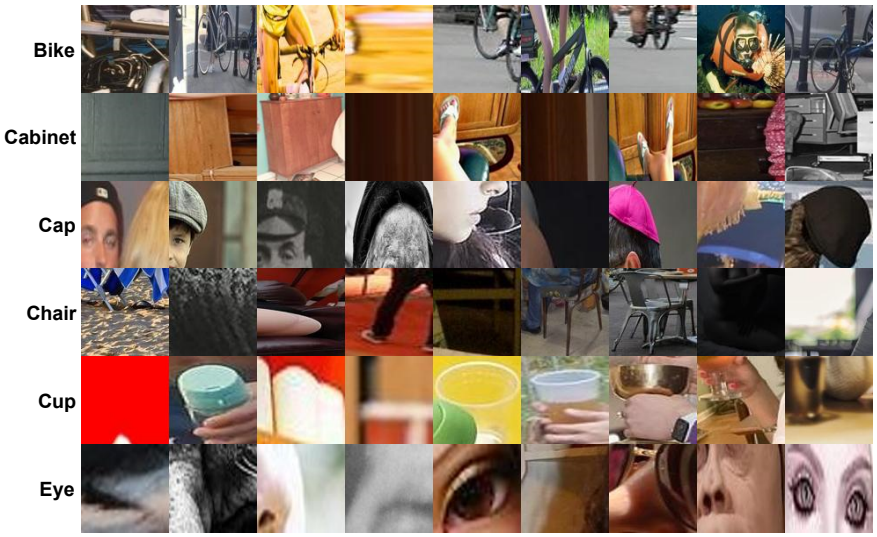

Fig. 2: Some objects in PRIVACY1000.

object. In the process of transforming the scene graph into a heterogeneous graph, we remove relationships with a confidence level below 0.5. This is done to avoid redundancy in the scene graph and reduce the disturbance of irrelevant information.

3.2 Graph Neural Network

In the Heterogeneous Graph Attention Network (HAN), Homogeneous Graph Attention Network (GAT), and Homogeneous Graph Convolution Network (GCN), we all adopt a two-layer convolution architecture. The dimension of the hidden layer for all models is set to 128. Specifically, the Heterogeneous Graph Attention Network (HAN) introduces a dual-head attention mechanism.

4 Model Training Details

4.1 Hyperparameters

During training, we use the Adam optimizer for model parameter optimization, and set the learning rate to 0.01 and weight decay to 0.0001 to prevent overfitting. Meanwhile, the training process will iterate over the entire dataset 200 times. In each iteration, the model will calculate the loss based on the predicted and actual results, and then use the optimizer to update the weights to minimize the loss.

4.2 Loss Function

During the training process, we use a custom loss function that includes L2 regularization. It consists of two parts: weighted binary cross-entropy loss and L2 regularization loss.

The weighted binary cross-entropy loss is defined as follows:

$$L_{BCE} = -w_1 \cdot y \cdot \log(pred) - w_0 \cdot (1 - y) \cdot \log(1 - pred) \tag{1}$$

The L2 regularization loss is defined as follows:

$$L_{reg} = \lambda_{reg} \cdot \sum_i ||param_i||_2^2 \tag{2}$$

Therefore, the total loss function is:

$$L_{total} = L_{BCE} + L_{reg} \tag{3}$$

During the training process, we first limit the predicted values between 0.0001 and 0.9999 to ensure numerical stability. Then, we use a weighted binary cross-entropy loss function, where w_1 and w_0 are the weights for the positive samples (privacy objects) and negative samples (public objects), respectively. Since in the scene graph, the number of public nodes is usually far greater than the number of privacy nodes, this may lead to an imbalance in the dataset. To solve this problem, we adjust the loss function by manually setting the weights of different objects, making w_1 greater than w_0, thus enhancing the model's focus on privacy objects. In addition, we calculate the L2 norm of all model parameters and include it in the total loss, achieving L2 regularization, where λ_{reg} is the regularization coefficient. This strategy helps prevent model overfitting and maintain the model's generalization ability.

5 Discussions and Limitations

One limitation of our work is that the accuracy of our proposed model is constrained by the accuracy of the scene graph generation model. Since privacy objects do not exhibit translation invariance, it is necessary for us to infer the features of the objects and the relationships between them, which requires the model to capture both scene and object features. However, some lower-quality scene graph generation models may have issues with sparse nodes and relationships, which restricts our SHAN model from accurately identifying privacy objects, leading to a decrease in detection accuracy.

Another limitation lies in the differing understandings of the concept of privacy in today's society, which was reflected in our process of creating the dataset. Even within our team, there were disagreements about the judgement of privacy objects in some images. We ended up adopting all objects that all team members considered to be private. This is mainly because there is no universally accepted, clear standard for judging privacy in the current social context.

With the continuous advancement of scene graph generation models, we anticipate improvements in the recognition accuracy of objects in images and the accuracy of relationships between objects, which will help enhance the accuracy of our SHAN model in privacy object detection tasks. Therefore, improving the accuracy of scene graph generation models and effectively utilizing scene graphs will be a major direction of our future research. In addition, formulating a clear standard for judging privacy is also an important task for our future research.

References

1. Zheng, Z., Wang, P., Ren, D., Liu, W., Ye, R., Hu, Q., Zuo, W.: Enhancing geometric factors in model learning and inference for object detection and instance segmentation. IEEE Transactions on Cybernetics **52**(8), 8574–8586 (2022). https://doi.org/10.1109/TCYB.2021.3095305